A USDOT NATIONAL UNIVERSITY TRANSPORTATION CENTER

Carnegie Mellon University

Penn
University of Pennsylvania

The Ohio State University

CCAC

Platooning for Improved Safety and Efficiency of Semi-Trucks (PISES-IV)

PI: Venkat Viswanathan
(https://orcid.org/0000-0003-1060-5495)

FINAL RESEARCH REPORT

Contract # 69A3551747111

Contents

1 Overview of Platooning

Platooning could be generally defined as two or more vehicles arranging themselves in a specific pattern to travel together. This leads to several benefits including improved safety for the drivers as well as improved overall efficiency of the vehicles involved [1]. The increase in efficiency is largely due to a reduction in aerodynamic drag experienced by the participating vehicles (including the lead vehicle) [2]. The configuration of the vehicles involved in the platoon is a degree of freedom that impacts the overall efficiency. A computational fluid dynamics study explored various configurations of medium-duty trucks in a platoon to determine the optimal configuration for overall platoon efficiency [3]. Based on the analysis, the study showed that one truck behind another in a single lane yields the greatest reduction in the average drag coefficient of about 23% [3]. Another study performed under the PATH project studied the effect of vehicle spacing and number of vehicles in a platoon on the average coefficient of drag of the entire platoon [4]. Using model vans, they determined the average drag coefficient in several configurations with different numbers of vehicles in the platoon and varying inter-vehicle spacing. The results for the drag coefficient reduction as a function of inter-vehicle spacing and number of trucks are shown in Figure 1, where vehicle spacing is the distance between the vehicles normalized by the length of a vehicle in the platoon.

The aforementioned PATH project study was performed using models of vans rather than semi-trucks and this raises the question of whether these results will still hold for semi-trucks. In order to validate the data shown in Figure 1, we compare the predicted aerodynamic drag utilizing the data from the study[3] against other studies [6, 7], as summarized in Figure 2. The benchmarking cases include (i) a study by NREL based on wind tunnel experiments to determine the drag of a platoon of two trucks relative to a single truck [6], and (ii) an experimental study exploring cab shapes comparing aerodynamics of a “clean” cab relative to an aerodynamically

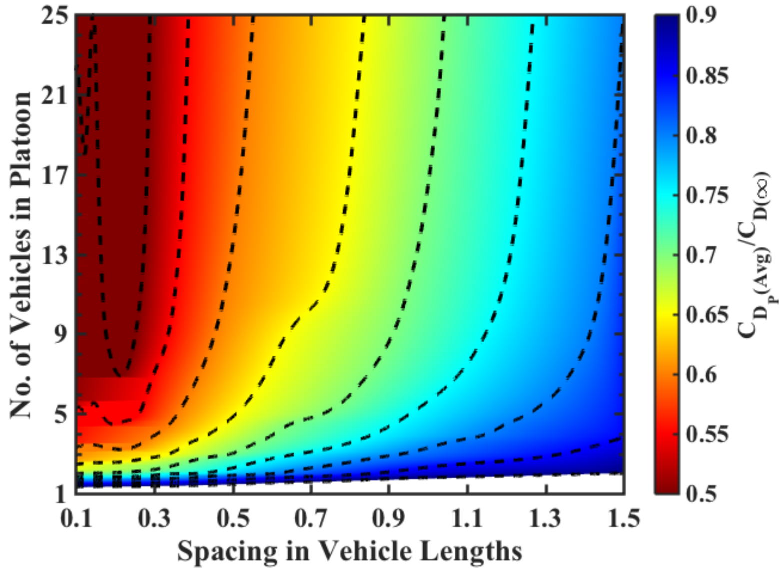

Figure 1: Average drag coefficient reduction per vehicle in the platoon as a function of the inter-vehicle spacing and the number of vehicles in the platoon. The drag coefficient reduction is expressed as the ratio of average drag coefficient of the platoon to the drag coefficient of a single vehicle. The inter-vehicle spacing is a normalized value that is determined by dividing the distance between the vehicles by the average vehicle length. We can observe that while significant improvements are obtained by increasing the number of vehicles from a single vehicle to a few vehicles, the improvements saturate after a certain number of vehicles. From ref. 5
.

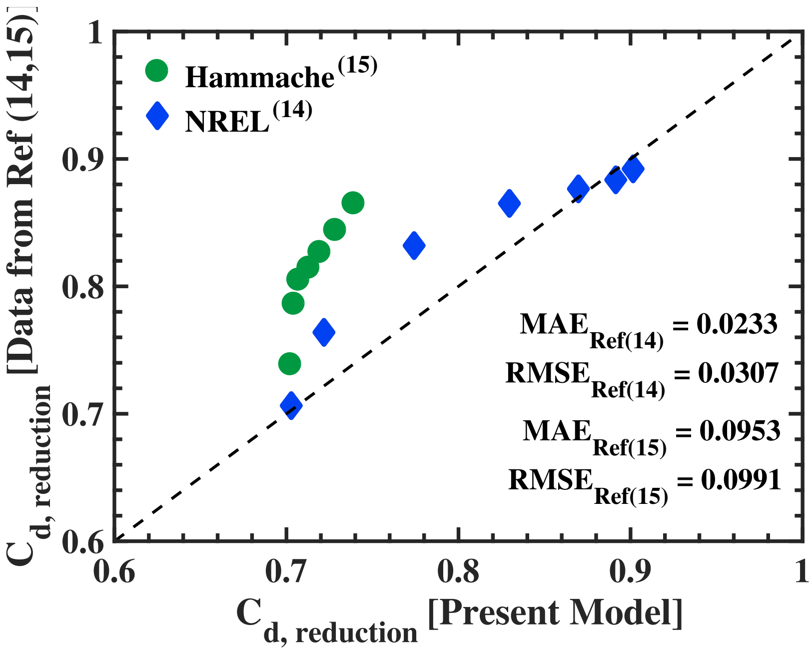

Figure 2: A comparison of the average drag coefficient reduction obtained from wind tunnel tests conducted by NREL [6] and Hammache et. al. [7]., ($C_{d,reduction}$[Data]), and the average drag coefficient reduction predicted by our model, ($C_{d,reduction}$[Present Model]), given the same initial parameters as each of the cases performed by the respective wind tunnel experiments. The dashed line represents the points where the predicted value exactly matches that of the corresponding experiment thus the farther away a value is from the line, the more inaccurate the prediction from the model is. From ref. 5

.

"dirty" cab [7]. For the cases considered, an average reduction in the coefficient of drag was determined meanwhile our model was used to predict the reduction in the average coefficient of drag using the same set up for each of the cases. The results are shown in Figure 2 and the dotted line represents perfect agreement between model and data. This figure shows that, in general, the model matched the NREL data [6] much better than the data from Hammache et al. [7] with an MAE and RMSE of 0.025 and 0.032 respectively compared to an MAE of 0.096 and an RMSE of 0.098. These values approximate the uncertainty for the potential drag coefficient reductions and shows that the model can be used to reasonably predict the average reduction in the drag coefficient for semi-truck platoons.

In the next chapter, we will explore more accurate drag coefficients beyond our previous work published in ref. 5.

2 The Effect of Platooning with more accurate drag coefficients

Incepts' [8] dynamic modeling of the vehicle and the batteries allow it to capture the impact that the environment has on the performance of the vehicles. One aspect of the vehicle model that can be improved is the drag coefficient. Since Incepts has information on the wind velocity and the direction of the wind, Incepts can utilize a dynamic drag coefficient that is dependent upon the oncoming wind conditions to better estimate the resulting power requirements. In this project, we utilized Incepts' dynamic models, with the additional dynamic drag coefficient algorithm, to better understand how their platooning trucks perform under realistic conditions.

2.1 High-fidelity Vehicle Model

Building on the 1D vehicle power model (Eq. 1), we introduced a variable drag coefficient C_d, to account for the effects of platoon position (i), vehicle spacing (Δ_v), wind speed ($\vec{v}_{wr}$).

$$\begin{aligned} F_g &= C_{rr} mg \sin Z + mg \cos Z \\ F_a &= (m + I/r)\vec{a} \cdot \hat{x} \\ F_w &= \frac{1}{2} C_d \rho A (\vec{v}_{wr} \cdot \vec{v}_v) \times \|\vec{v}_{wr}\| \times \|\vec{v}_v\| \\ P &= \left(F_g + F_a + F_w\right) \vec{v}_v \cdot \hat{x} + P_{aux} \end{aligned} \tag{1}$$

$$C_d = f(i, \vec{v}_v, \vec{v}_w, \Delta_v, \ldots) \tag{2}$$

The overall power draw of the platoon is then the sum of each individual vehicle's power (Eq. 3), computed using a platooning aware $C_{d,i}$. We treated the platoon as a point mass centered on the lead vehicle, thus neglecting variable environmental conditions (i.e. road grade) along the platoon. For the platoons' sizes considered, we expect this to be a reasonable approximation.

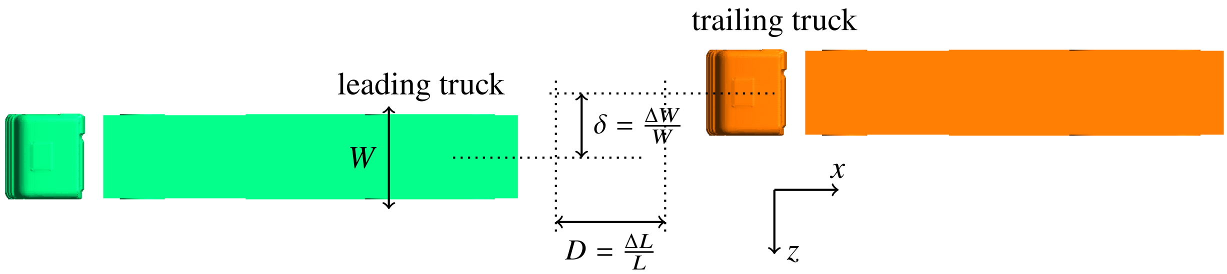

Figure 3: Definition for following distance D and following offset δ. Following distance $D = \frac{\Delta D}{L}$, where ΔD is the distance from the back of the first truck to the front of the second truck and L is the length of the truck in x direction. Following offset $\delta = \frac{\Delta W}{W}$, where ΔW is the distance between the center line of two trucks in z direction and W is the width of truck.

$$P = \sum P_i \left(C_{d,i}(i, \vec{v}_v, \vec{v}_w, \Delta_v, ...)\right) \tag{3}$$

In order to develop a model for C_d over a wide range of operating conditions (Table 1), a series of computation fluid dynamics (CFD) simulations of platoons of trucks in single vehicle and platoon configurations have been performed using a method (variational multiscale method (VMS)) that is comparable to Large Eddy Simulations (LES). This well-validated approach provides a higher fidelity flow physics simulation compared to conventional RANS type models [9, 10]. In this case, a standard box vehicle was chosen with a highway driving speed of 55 miles per hour in addition to the wind conditions. The results from these CFD computations are shown in Figure 4a.

As was done in the original Incepts work [8], the wind and temperature data came from the NREL Windtool Kit and were recorded on 12/21/15 at 12:00 pm [11, 12, 13, 14] while the elevation data came from the USGS national elevation map [15]. The wind speed was taken at 10 meters altitude while the air temperature was taken from 2 meters altitude both of which are the closest to the surface heights for those particular attributes offered through the NREL data set. The drive cycle used throughout this analysis was the EPA Highway drive profile (HWFET) [16]. Since this drive cycle was repeated multiple times throughout the route, the

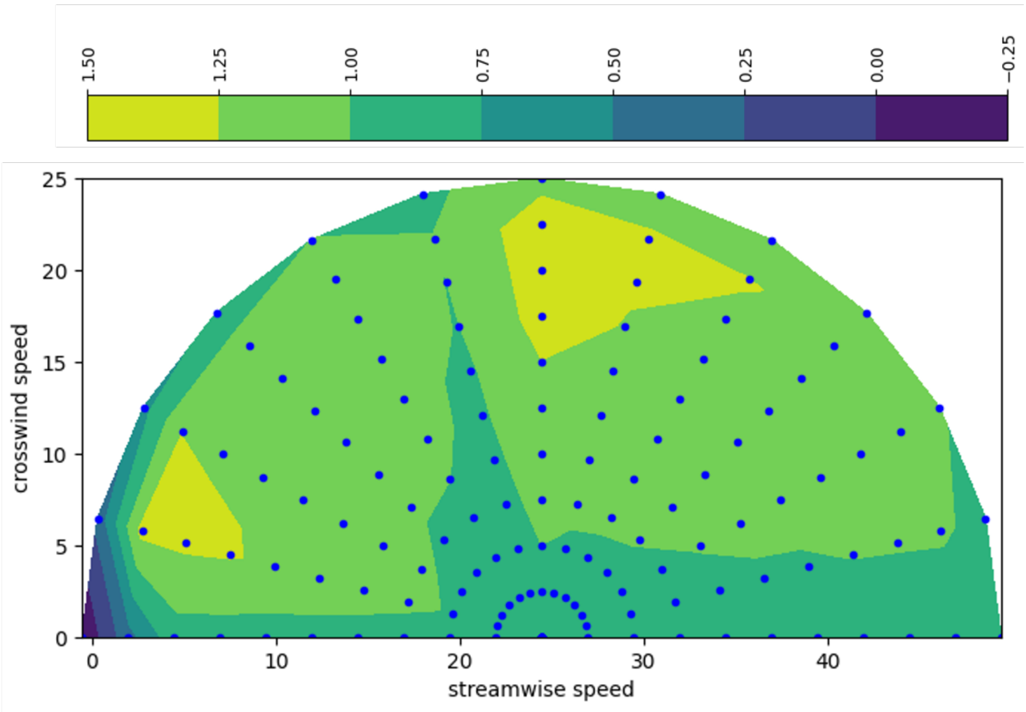

(a) Variable Truck Drag Coefficient

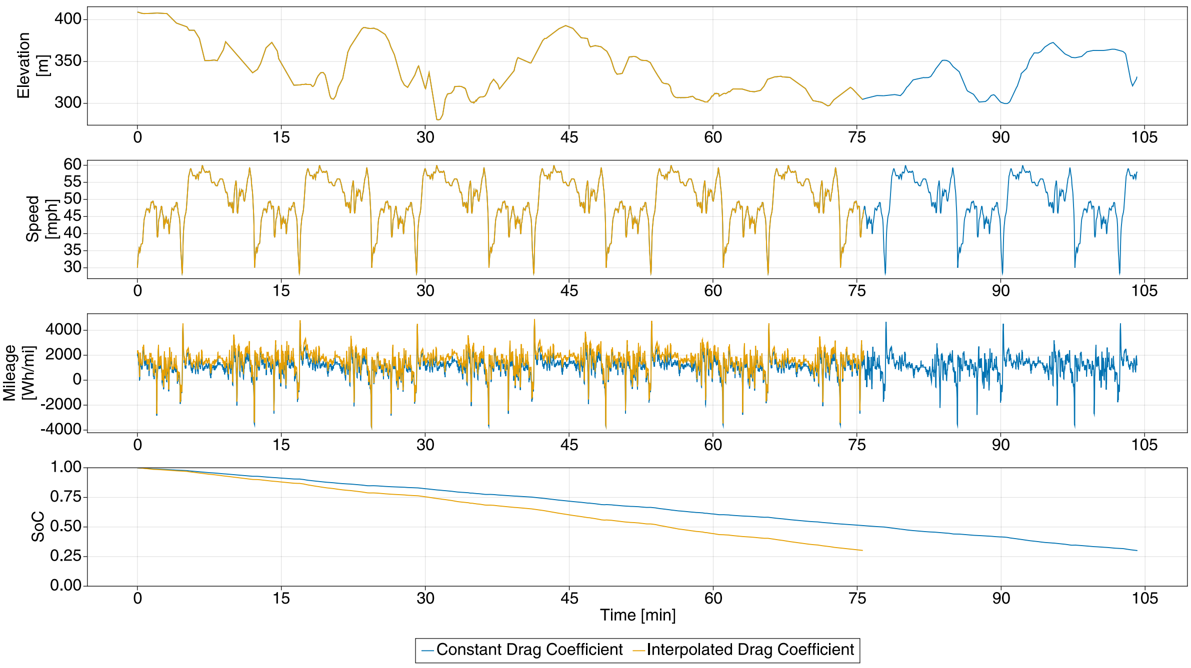

(b) Power consumption with and without a variable C_d

Figure 4: Using a constant Drag Coefficient underestimates energy consumption by ~40%

tails of this drive cycle were trimmed such that the input drive cycle starts and ends around 30 mph. To directly compare the impact of the dynamic drag coefficient, both sets of simulations utilized the exact same route. The results from both simulations are shown in Figure 4 along with the drag coefficient variability as a function of the streamwise speed (head wind) and crosswind speed. As shown by this figure, the simulation using the dynamic drag coefficient reached the threshold SoC, which was set to 30%, nearly 30 minutes less into the route than the constant drag coefficient simulation. This amounts to an underestimation in energy consumption by 40%. This demonstrates the importance of incorporating dynamic drag coefficients into electric vehicle simulations as this will drastically impact the energy requirements, and thus the infrastructure/safety recommendations made using this information.

Parameter	Range		Unit
Vehicle Speed	0	70	mph
Wind Speed	0	60	mph
Normalized Vehicle Spacing	0.05	2	—
Wind Angle	0	180	°
Number of Trucks	1	4	—
Lateral Offset	-7	7	ft

Table 1: The explored variables and ranges for the drag coefficient CFD simulations

3 Future Work

3.1 Surrogate Model of CFD Platoon Drag Coefficients

Future CFD simulations will use a representative truck model, ideally provided by Locomation, or an internally developed representative model. The various geometries, including number of vehicles, vehicle spacing (D) and lateral offset (δ) are shown in Figure 3. Different boundary conditions, such as vehicle speed, wheel rotation and apparent wind are included in the simulation.

The rectilinear limits outlined in Table 1, were set to fully bound the feasible range of operating conditions. We expect that platooning will provide marginal benefits for some regions of the proposed domain (ie. low speeds, orthogonal cross-winds). However by capturing these points we will be able to identify the regions, that do matter, with greater fidelity.

3.1.1 Adaptive Sampling of Domain

Grid sampling over the operating domain is infeasible given the high dimensionality of the domain, and high compute cost of a single CFD simulation. Even with only 5 sample points along each dimension, we would need $5^6 \rightarrow 15,625$ simulations. Further, prior research shows diminishing returns as Δ_v increases, thus even sampling over the entire domain would be inefficient [5].

We will utilize an adaptive sampling tool, to guide the sampling of CFD simulations needed to create the surrogate model. This tool will be based on an asynchronous Bayesian sampling based approach that can efficiently sample moderate (3-30) dimensional spaces [17]. The tool can orchestrate submission and execution of individual CFD simulations across HPC resources and can direct simulations towards regions of maximal expected improvement [18]. Sampling will continue until the expected root-mean-sum-square (RMSS) error in C_d over the entire domain is less than 1‰, or 20 million core-hours, whichever comes first.

3.1.2 Surrogate Model

Using the generated database of platooning drag coefficients, the Viswanathan Team will build a surrogate model for the functional form of Eq. 2. This surrogate model will be a linear interpolant, Multi-Layer Preceptron, or the underlying model used in 3.1.1. The final model selection will be based on the Bayesian Information Criteria of the examined surrogates [19].

3.2 Platooning Case Studies

We proposed using the above tool to simulate platoons of trucks traveling along the routes outlined in Table 2. These routes were selected to highlight regions where platooning is likely important (Kansas City to Oklahoma City) and regions where other effects such as traffic (Providence to Greenport) or elevation (Salt Lake City to Denver) are expected to dominate. Simulations were conducted for the full range of platoon sizes and vehicle spacing as outlined in Table 1.

3.2.1 Sensitivity Analysis

As Incepts is built on Julia's Scientific Machine Learning Ecosystem, simulation results are fully differentiable with respect to their input parameters.

This capability can be leveraged to compute the sensitivity of the platoon's consumption

Route		Distance [mi]	Elevation Change [ft]
Providence, Rhode Island	Greenport, New York	256	1k
Salt Lake City, Utah	Denver, Colorodo	517	19k
Kansas City, Missouri	Oklahoma City, Oklahoma	350	4k

Table 2: Proposed Case Studies for Platooning Simulation

to vehicle spacing ($\delta E/\delta\Delta_v$), for the proposed routes. This is a key performance metric for autonomous platooning, as it will factor into the design of the vehicle control system, and any trade offs between safety (more space) and fuel efficiency (less space).

Further, we can compute the sensitivity with respect to vehicle alignment offsets (i.e. how well the vehicles follow each other). Again this is a key performance metric for autonomous platooning, as it sets the trade-offs between maintaining the configuration and the vehicle's power requirements.

Appendix: Symbols

Symbol	Term	Unit
P	Vehicle Power	W
P_{aux}	Non-locomotion Power Consumption	W
F_a	Vehicle Acceleration	N
F_g	Ground Reaction Force	N
C_{rr}	Rolling Resistance	
F_w	Aerodynamic Drag	N
m	Vehicle Mass	kg
$\hat{x}$	Unit Vector align longitudinally with the vehicle	
I	Moment of Inertia of the vehicle	$kg \cdot m^2$
r	Effective radius of rotating inertia wrt. vehicle speed	m
$\vec{v}_v$	Velocity of the Vehicle	m/s
$\vec{v}_{wr}$	Velocity of Wind rel. vehicle	m/s
$\vec{a}$	Vehicle Acceleration	m/s^s
Z	Road Grade	
Δ_v	Vehicle Spacing	m
C_d	Aerodynamic Drag Coefficient	
A	Drag area of vehicle	m^2
g	Standard Gravity	m/s^2
ρ	Air Density[1]	kg/m^3

References

[1] A. Alam, B. Besselink, V. Turri, J. Martensson, and K. H. Johansson, "Heavy-duty vehicle platooning for sustainable freight transportation: A cooperative method to enhance safety and efficiency," *IEEE Control Systems*, vol. 35, no. 6, pp. 34–56, 2015.

[2] J. Patten, B. McAuliffe, W. Mayda, and B. Tanguay, "Review of aerodynamic drag reduction devices for heavy trucks and buses," *National Research Council Canada NRC Technical Report CSTT-HVC-TR*, vol. 205, 2012.

[3] P. Vegendla, T. Sofu, R. Saha, M. M. Kumar, and L.-K. Hwang, "Investigation of aerodynamic influence on truck platooning," *SAE Technical Paper*, pp. 2015–01–2895, 2015.

[4] M. Zabat, N. Stabile, S. Farascaroli, and F. Browand, "The aerodynamic performance of platoons: A final report," california path research report, ucb-its-prr-95-35, Institute of Transportation Studies, University of California, Berkeley, 1995.

[5] M. Guttenberg, S. Sripad, and V. Viswanathan, "Evaluating the Potential of Platooning in Lowering the Required Performance Metrics of Li-Ion Batteries to Enable Practical Electric Semi-Trucks," *ACS Energy Letters*, vol. 2, pp. 2642–2646, Nov. 2017.

[6] K. Salari, "Doe's effort to improve heavy vehicle fuel efficiency through improved aerodynamics." https://energy.gov/sites/prod/files/2016/06/f33/vs006_salari_2016_o_web.pdf, 2016. Online Article, Accessed Date: 20-September-2017.

[7] M. Hammache, M. Michaelian, and F. Browand, "Aerodynamic forces on truck models, including two trucks in tandem," *SAE Technical Paper*, pp. 2002–01–0530, 2002.

[8] M. Guttenberg, S. Sripad, A. Bills, and V. Viswanathan, "INCEPTS: Software for high-fidelity electric vehicle en route state of charge estimation, fleet analysis and charger deployment," *eTransportation*, vol. 7, p. 100106, Feb. 2021.

[9] K. Saurabh, B. Gao, M. Fernando, S. Xu, M. A. Khanwale, B. Khara, M.-C. Hsu, A. Krishnamurthy, H. Sundar, and B. Ganapathysubramanian, "Industrial scale large eddy simulations with adaptive octree meshes using immersogeometric analysis," *Computers & Mathematics with Applications*, vol. 97, pp. 28–44, 2021.

[10] K. Saurabh, M. Ishii, M. Fernando, B. Gao, K. Tan, M. Hsu, A. Krishnamurthy, H. Sundar, and B. Ganapathysubramanian, "Scalable adaptive pde solvers in arbitrary domains," in *Super Computing*, 2021.

[11] C. Draxl, B. Hodge, A. Clifton, and J. McCaa, "Overview and meteorological validation of the wind integration national dataset toolkit," tech. rep., National Renewable Energy Lab.(NREL), Golden, CO (United States), 2015.

[12] C. Draxl, A. Clifton, B.-M. Hodge, and J. McCaa, "The wind integration national dataset (wind) toolkit," *Applied Energy*, vol. 151, pp. 355–366, 2015.

[13] W. Lieberman-Cribbin, C. Draxl, and A. Clifton, "Guide to using the wind toolkit validation code," tech. rep., National Renewable Energy Lab.(NREL), Golden, CO (United States), 2014.

[14] J. King, A. Clifton, and B.-M. Hodge, "Validation of power output for the wind toolkit," tech. rep., National Renewable Energy Lab.(NREL), Golden, CO (United States), 2014.

[15] D. Gesch, G. Evans, J. Mauck, J. Hutchinson, W. J. Carswell Jr, *et al.*, "The national map—elevation," *US geological survey fact sheet*, vol. 3053, no. 4, 2009.

[16] EPA, ""Dynamometer Drive Schedules"." https://www.epa.gov/vehicle-and-fuel-emissions-testing/dynamometer-drive-schedules#vehicleDDS, 2017. Accessed Date: 20-September-2019.

[17] B. S. S. Pokuri, A. Lofquist, C. M. Risko, and B. Ganapathysubramanian, "Paryopt: A software for parallel asynchronous remote bayesian optimization," *arXiv preprint arXiv:1809.04668*, 2018.

[18] T. J. Mackman, C. B. Allen, M. Ghoreyshi, and K. J. Badcock, "Comparison of Adaptive Sampling Methods for Generation of Surrogate Aerodynamic Models," *AIAA Journal*, vol. 51, pp. 797–808, Apr. 2013.

[19] S. Watanabe, "A Widely Applicable Bayesian Information Criterion," *arXiv:1208.6338 [cs, stat]*, Aug. 2012.